Chapter 5

Extended serial setup

Chapter 4 is dedicated to a serial shaper setup, which is based on a confinement of arrays with the optical axis of the crystals aligned at 45° or −45° with respect to the polarization of the incoming light. As demonstrated, multipass solutions with such an array configuration limit the polarization manipulation capabilities. In this chapter the potential of using arrays with rotated optical axes is anticipated. This additional degree of freedom becomes useful and it allows to add the missing piece of the serial solution, namely the control over the relative phase shift between the P and S components to the new setup.

In the first Section different relative orientations of the liquid crystals are analyzed. Afterwards, the compositions of a three layer phase and polarization modulator are discussed [41]. Then a four layer modulator capable of full polarization, phase, and amplitude control is introduced. In order to achieve a similar configuration of liquid crystals optical axes as a four layer modulator, but with the double array modulator, a new multipass layout is proposed. The use of waveplates in between the following passes of a shaper allows to rotate the relative ordination of the otherwise crossed arrays. Finally, the influence of the grating polarization efficiency is studied for both layouts.

5.1 Modeling the crystal optical axis orientation

Polarization shaping obtained by interaction of the P polarized light with one layer of nematic crystals with their axis orientated at 45° with respect to the P plane is restricted. The resulting states of polarization are described by the vector $\begin{bmatrix} \cos[\frac{\phi}{2}] \\ i\sin[\frac{\phi}{2}] \end{bmatrix}$. The controlled parameter here is the relative amplitude of the created P and S polarization components with the relative phase between them fixed to $\frac{\pi}{2}$. This state corresponds to an ellipse with principal axes along the P or S direction. Thus, the choice of the principal axes ratio fully determines the spectral polarization state and there is no possibility of changing the polarization ellipse orientation. The cause for this restriction is the fixed phase shift between the P and S polarization components. Once the relative phase shift can be changed, the control over the polarization would be complete.

The control over the amplitude of orthogonal polarization components and their relative phase shift is obtained by a different choice of optical axes orientation in the following arrays. The concept is to create both polarization components in the first array and shift the relative phase in the second. Equation 5.1 describes the Jones vector of the polarization obtained after an array with optical axis orientated at an angle θ.

$$M_\theta[\phi] \cdot P = \begin{bmatrix} \cos[\frac{\phi}{2}] + i\cos[2\theta]\sin[\frac{\phi}{2}] \\ i\sin[2\theta]\sin[\frac{\phi}{2}] \end{bmatrix} \tag{5.1}$$

In order to change the relative amplitude of the components in the full range, the orientation has to be set to $45° \pm 90°$. Other settings do not allow to generate a pure S polarization component or extinguishing the P component. Afterwards, the polarization components created in this rotated array, could be shifted in phase by the following array. Since the shift of the components should be independent, the possible orientations are along the P or S direction. In the case of the second array orientated parallel, as shown on Figure 5.1, the P component would undergo a variable extraordinary index of refraction, whereas the S component would experience ordinary refraction.

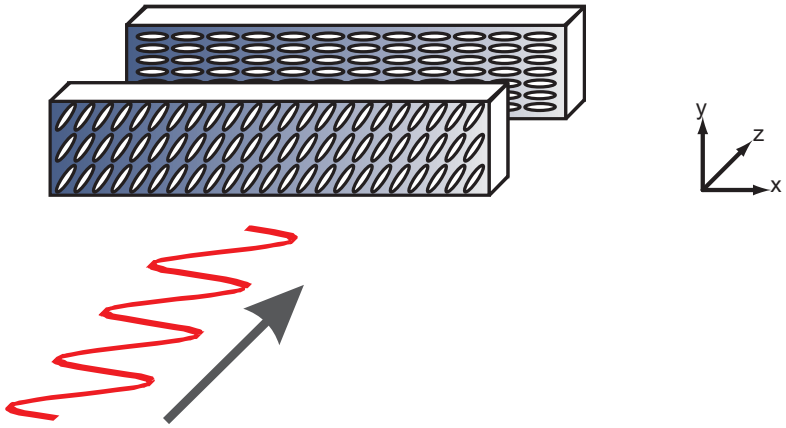

Figure 5.1: Arrangement of two arrays of crystals. The optical axes are orientated at 45° for the first array and 0° for the second.

$$M_{0^\circ}[\phi_b] \cdot M_{45^\circ}[\phi_a] \cdot P = e^{\frac{1}{2}i\phi_a} \begin{bmatrix} e^{i\phi_b} \cos[\frac{\phi_a}{2}] \\ i \sin[\frac{\phi_a}{2}] \end{bmatrix} \tag{5.2}$$

The retardance of the first array ϕ_a regulates the relative amplitudes of the components and by changing the retardance of the second array ϕ_b, the relative phase is shifted. Moreover, by combining a phase and amplitude modulator with a phase modulator as presented on Figure 5.2 it is possible to fully control the spectral polarization as well as the phase of the pulse.

The spectral phase and the polarization components are formed by the first two arrays as described earlier in Chapter 4. The third array with parallel orientation of crystal optical axes allows to regulate a relative phase shift as Vector 5.3 indicates.

$$M_{0^\circ}[\phi_c] \cdot M_{-45^\circ}[\phi_b] \cdot M_{45^\circ}[\phi_a] \cdot P = e^{\frac{1}{2}i(\phi_a+\phi_b)} \begin{bmatrix} e^{i\phi_c} \cos[\frac{\phi_a-\phi_b}{2}] \\ i \sin[\frac{\phi_a-\phi_b}{2}] \end{bmatrix} \tag{5.3}$$

This concept was first presented theoretically and experimentally by the group of Y. Silberberg [41] with the use of components commercially available on the market.

The above presented construction is very interesting, but given the freedom of constructing the phase and polarization spatial light modulator, other

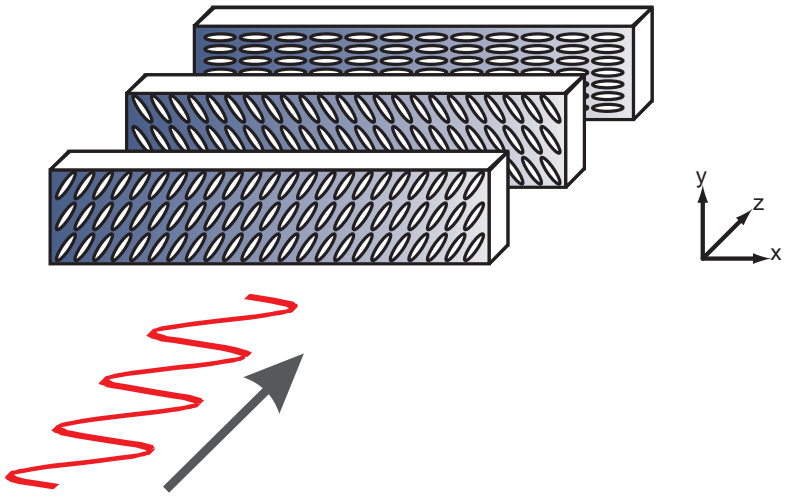

Figure 5.2: Arrangement of three arrays of crystals equivalent to a combined phase and amplitude modulator with a phase modulator. The optical axes in the following arrays are orientated at 45°, −45°, and 0°.

options seems to be more attractive. Let us consider the relative shift of polarization components caused by the parallel, 0° orientated array. The phase shift of the P component is controlled by altering of the extraordinary index of refraction while the S phase remains unchanged. When this modulator is used for extremely short pulses, the initial difference[1] of the optical path of those components should be smaller than the accessible range within the extraordinary (P) path can be scanned. In other words, the condition $|(n_e - n_o)| < |\Delta n_e|$ has to be fulfilled. Otherwise, the offset phase shift may cause the whole P polarization pulse to be shifted in time with regard to the S polarized pulse. For the thin crystals this effect can be neglected, but there are other solutions that are free of this effect. The design demonstrated in Figure 5.3 contains arrays of crystals aligned at 45°, 0°, and 90°.

$$M_{90^\circ}[\phi_c] \cdot M_{0^\circ}[\phi_b] \cdot M_{45^\circ}[\phi_a] \cdot P \;=\; e^{\frac{1}{2}i\phi_a} \begin{bmatrix} e^{i\phi_b} \cos[\frac{\phi_a}{2}] \\ i\, e^{i\phi_c} \sin[\frac{\phi_a}{2}] \end{bmatrix} \tag{5.4}$$

It is superior to the previous crystal sandwich, while both components undergo the extraordinary and ordinary index of refraction. In consequence,

[1]The situation when no voltages are applied on the crystal arrays

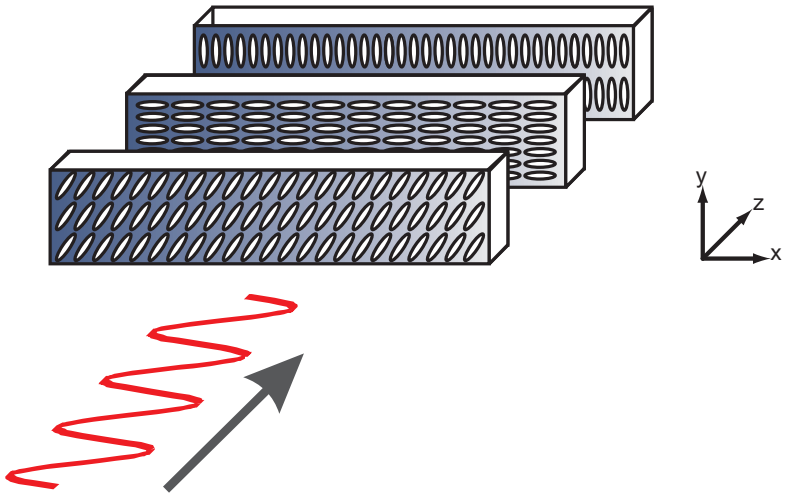

Figure 5.3: Arrangement of three arrays of crystals. The optical axes in the following arrays are orientated at 45°, 0° and at 90°.

for this modulator for $\phi_b = \phi_c$, the relative phase shift is independent of the difference between extraordinary and ordinary index of refraction.

At this point the missing parameter is the amplitude modulation, which in the phase and amplitude shaper is achieved by using a polarizer. Therefore an array of 45° orientated crystals fused with a parallel polarizer is placed as a first element in a four array modulator, as it is shown in Figure 5.4.

The corresponding vector (5.5), shows that the absolute amplitude can be controlled as well as the ratio of the two polarization components.

$$M_{90^\circ}[\phi_d] \cdot M_{0^\circ}[\phi_c] \cdot M_{45^\circ}[\phi_b] \cdot PP \cdot M_{45^\circ}[\phi_a] \cdot P = \cos[\frac{\phi_a}{2}]\, e^{\frac{1}{2}i(\phi_a+\phi_b)} \begin{bmatrix} e^{i\phi_c}\cos[\frac{\phi_b}{2}] \\ i\, e^{i\phi_d}\sin[\frac{\phi_b}{2}] \end{bmatrix} \tag{5.5}$$

It is important to point out that for this configuration the amplitudes E_{0x} and E_{0y} and the phases φ_x and φ_y can be manipulated independently of each other for both polarization components, thus full control of the polarization, amplitude an phase is accomplished.

$$E_{0x}(\phi_a, \phi_b) = \cos\left(\frac{\phi_a}{2}\right)\cos\left(\frac{\phi_b}{2}\right)$$

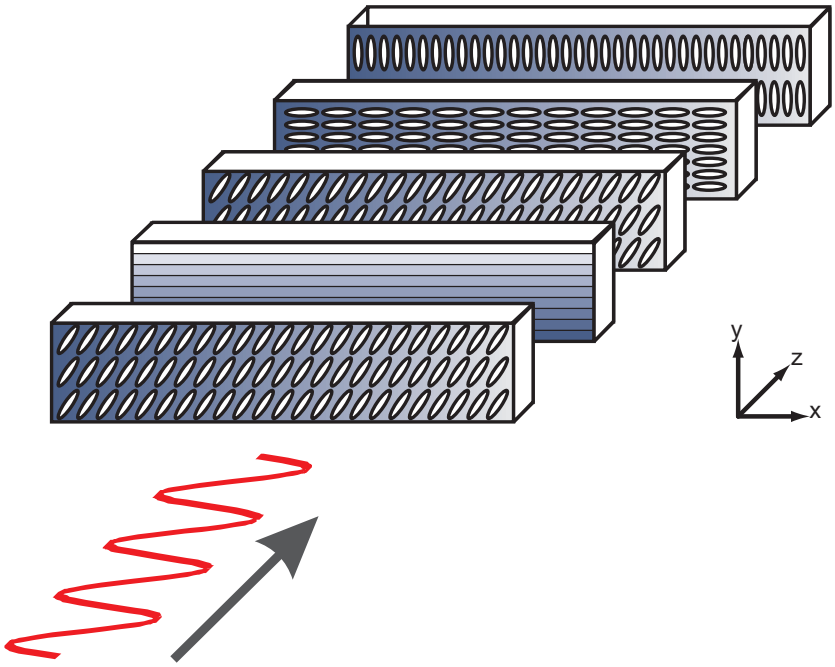

Figure 5.4: Arrangement of four arrays of crystals and a P orientated polarizer. The elements are ordered as follows: Array of crystals orientated at 45°, P polarizer, arrays at 45°, 0° and at 90°.

$$E_{0y}(\phi_a, \phi_b) = \cos\left(\frac{\phi_a}{2}\right) \sin\left(\frac{\phi_b}{2}\right) \tag{5.6}$$

$$\varphi_x = \frac{1}{2}(\phi_a + \phi_b) + \phi_c$$

$$\varphi_x = \frac{1}{2}(\phi_a + \phi_b) + \phi_d + \frac{\pi}{2} \tag{5.7}$$

This all could be achieved without facing the problems caused by interferometric instability of the setup, as in the parallel approach, but grants the same possibilities, full control over the phase, the amplitude, and the polarization. An example of such a setup is displayed in Figure 5.5

As described in Section 4.3, the efficiency of the grating is polarization sensitive and it tends to generate an unwanted amplitude modulation depending on the polarization. Applying the procedure introduced in Section 4.3 yields the Jones vector of a four array shaper with the grating.

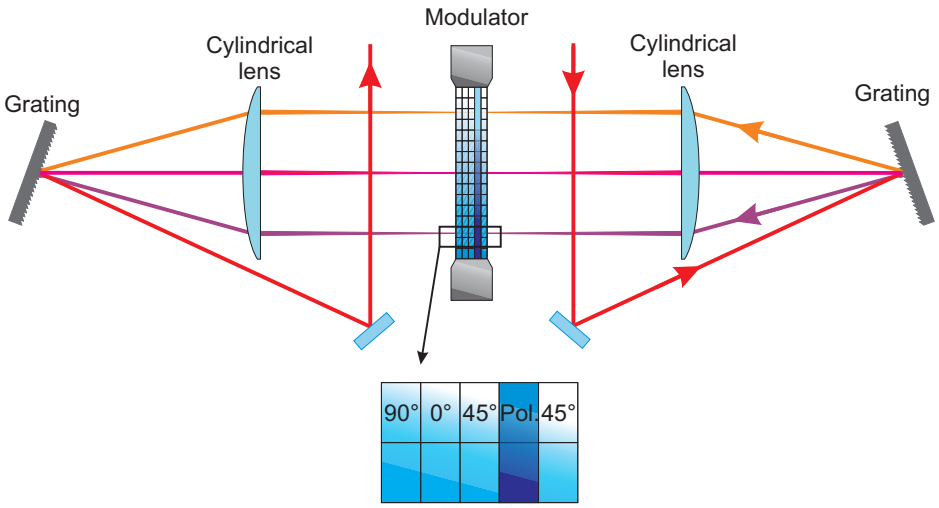

Figure 5.5: Four array modulator placed in the 4f setup.

$$G \cdot M_{90°}[\phi_d] \cdot M_{0°}[\phi_c] \cdot M_{45°}[\phi_b] \cdot PP \cdot M_{45°}[\phi_a] \cdot P = \cos[\frac{\phi_a}{2}]\, e^{\frac{1}{2}i(\phi_a+\phi_b)} \begin{bmatrix} e^{i\phi_c}\cos[\frac{\phi_b}{2}] \\ i\,g\,e^{i\phi_d}\sin[\frac{\phi_b}{2}] \end{bmatrix} \tag{5.8}$$

The relative amplitudes of the components of Vector 5.8 are modified in the same way as Vector 4.11, therefore the amplitude filter function 4.13 can be used to correct this effect. This returns the grating corrected Jones vector in the same form according to the arguments as used Section 4.3.

The introduced four arrays modulator could easily replace the phase and amplitude two array models with no changes to the existing classic 4f-setups. It offers the full possibilities of pulse shaping like the parallel setup with slightly lower efficiency due to the grating issue, but without problems with stability and complicated alignment.

5.2 Multipass shaper

Until four array modulators will be available, one can use existing modulators to yield similar functions. The described serial arrangement in Section 4 allows to modulate the amplitude and creates polarization components with a fixed relative phase. Adding an extra pass through the modulator will

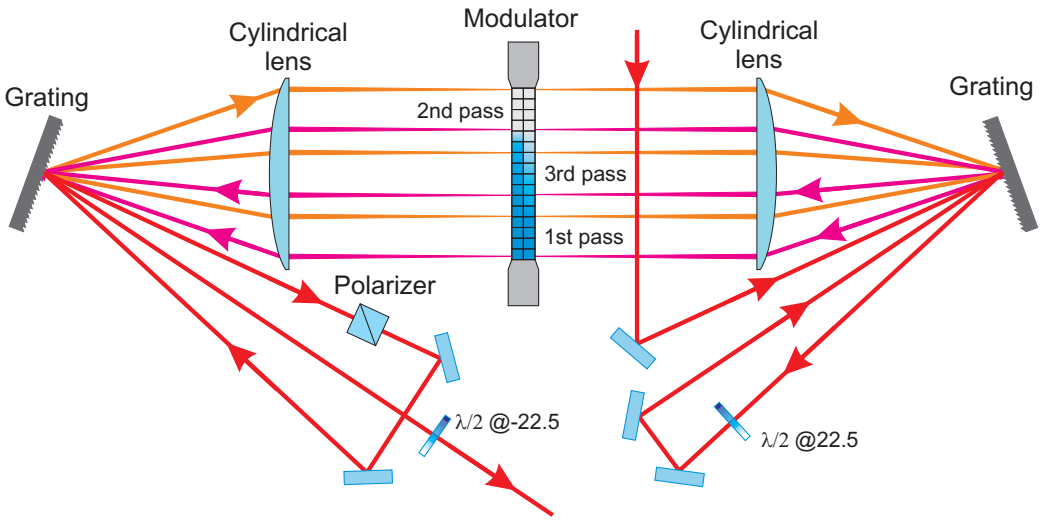

Figure 5.6: Three pass configuration of a serial shaper. The laser beam enters the first grating, as the arrow indicates, its spectral components are spatially separated and collimated by a cylindrical lens. Then they are transmitted through the modulator and hit the second grating. Afterwards, the beam is sent through the polarizer and is redirected again on the second grating at a different incident angle. The spectral components are sent a second time through another part of the modulator, and they enter the first grating for the second time. Next, the polarization of the beam is rotated by 45° by a waveplate and then the beam is sent the third time through the 4f-setup. As it leaves after third time, the polarization is rotated by −45°.

not offer any more options, unless the polarization state after the second pass is rotated. This corresponds to a relative rotation of the optical axis of the arrays in the third pass. Placing a half waveplate after the second pass and rotating the polarization state by 45° is equivalent to using the crystals orientated at 0° and 90° at the third pass. The example of this multipass shaper is shown in Figure 5.6

For simplicity of the calculations let us introduce the matrices of two elements: a double array modulator $M[\phi_x, \phi_y]$ where optical axes are rotated by 45° and −45°, respectively, and a half waveplate $HL[\theta]$, orientated at angle θ.

$$M_{3pass} = HL[-22.5°] \cdot M[\phi_e, \phi_f] \cdot HL[22.5°] \cdot$$

$$M[\phi_c, \phi_d] \cdot PP \cdot M[\phi_a, \phi_b] \cdot P =$$
$$\cos[\frac{\phi_a - \phi_b}{2}]\, e^{\frac{1}{2}i(\phi_a+\phi_b+\phi_c+\phi_d)} \begin{bmatrix} e^{i\phi_e} \cos[\frac{\phi_c-\phi_d}{2}] \\ i\, e^{i\phi_f} \sin[\frac{\phi_c-\phi_d}{2}] \end{bmatrix} \tag{5.9}$$

The introduced Vector 5.9 for the three pass setup resembles the vector 5.5 for the four array modulator. Indeed, when setting the differences $\phi_c - \phi_d$ and $\phi_a - \phi_b$ as parameters the vector has the identical form. Potentially, it has same capabilities as a four array modulator. Unfortunately, this is not the case. There are three major disadvantages of the three pass solution.

First of all, the spectrum is passing the modulator three times through different regions of the modulator in every pass. This makes the achievable shaper resolution at least three times smaller than in case of using a single pass 4f arrangement.

The multipass setup has as well its impact on the outgoing beam profile. The use of a cylindrical telescope off the optical axis leads to abberations like coma, astigmatism, and other beam distortions. Therefore, if the beam quality is an issue, this solution is not recommended.

The last issue is associated with the grating efficiency. The beam gets reflected six times by the gratings, therefore the overall efficiency of this shaper is much lower in comparison to a single pass.

Furthermore, the polarization sensitive grating efficiency has a strong impact on the pulse polarization and intensity in case of this setup. Polarization components other then pure P are created in the shaper in the second pass. Therefore, this effect can be debated from the third reflection on the first grating. The unequal reflectivity of the grating at the fourth bounce can be balanced by rotating the polarization by 90° before the fifth bounce, as shown in Figure 5.7. Afterwards, the polarizations components are turned by 45° in order to be aligned parallel and perpendicular to the optical axes of the crystals in the modulator. After passing the modulator for the third time, the waveplates turns back the polarization by −45°. The Jones vector of this arrangement is similar to 5.8.

$$M_{3pass} = G \cdot HL[-22.5°] \cdot M[\phi_e, \phi_f] \cdot HL[22.5°] \cdot$$
$$G \cdot HL[45°] \cdot G \cdot M[\phi_c, \phi_d] \cdot PP \cdot M[\phi_a, \phi_b] \cdot P =$$

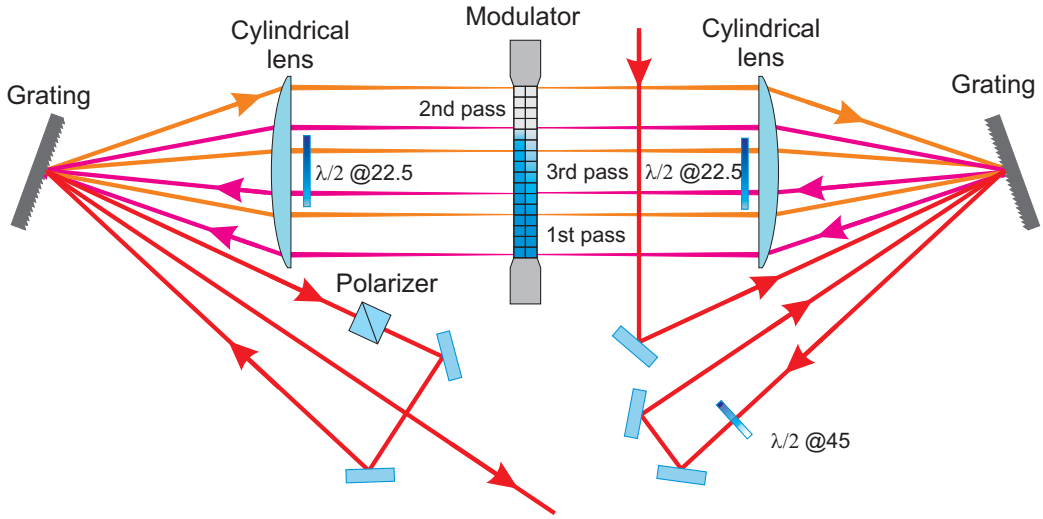

Figure 5.7: The three pass configuration of a shaper with additional wave-plates to correct the grating polarization sensitive reflectivity. The laser beam enters the first grating, as the arrow indicates, and its spectral components are spatially separated and collimated by the cylindrical lens. Then they are transmitted through the modulator and hit the second grating. Next, the beam is sent through the polarizer and is redirected again on the second grating at a different incident angle. Then, the spectral components are sent a second time through another part of the modulator. Afterwards, they enter the first grating for the second time and the polarization is rotated by 90°. Next, the beam hits the first grating and the polarization is turned by 45°. Then, the beam is sent a third time through the 4f setup. Before it hits the second grating, the polarization is rotated by $-45°$.

$$g\cos[\frac{\phi_a-\phi_b}{2}]\,e^{\frac{1}{2}i(\phi_a+\phi_b+\phi_c+\phi_d)}\begin{bmatrix} e^{i\phi_e}\cos[\frac{\phi_c-\phi_d}{2}] \\ i\,g\,e^{i\phi_f}\sin[\frac{\phi_c-\phi_d}{2}]\end{bmatrix} \tag{5.10}$$

In comparison with the 4 array shaper the grating factor g appears as a multiplier of the amplitude of both components. Apart from that, the vector resembles Vector 5.8, therefore the same grating filter can be successfully applied.

5.3 Grating influence on the transmission, phase, and polarization

In the previous sections the influence of the grating in a multipass and a four array shaper was discussed. Since the Jones vector is similar for both cases, the four array modulator can be considered without losing its universality.

This section describes the relation between the retardances written on the four arrays modulator and the resulting transmission, phase, and polarization ellipse parameters, the ratio r and the orientation γ.

The resulting Jones vector is in the form

$$\cos[\frac{\phi_a}{2}]\,e^{\frac{1}{2}i(\phi_a+\phi_b)}\begin{pmatrix} e^{i\phi_c}\cos[\frac{\phi_b}{2}] \\ i\,g\,e^{i\phi_d}\sin[\frac{\phi_b}{2}]\end{pmatrix}$$

from which the amplitudes of the polarization components are

$$E_{0x}(\phi_a,\phi_b)=\cos\left(\frac{\phi_a}{2}\right)\cos\left(\frac{\phi_b}{2}\right)$$

$$E_{0y}(\phi_a,\phi_b)=g\,\cos\left(\frac{\phi_a}{2}\right)\sin\left(\frac{\phi_b}{2}\right)\ , \tag{5.11}$$

where E_{0x} and E_{0y} corresponds to the P and S component respectively.

$E_{0y}(\phi_a,\phi_b)$ cannot be changed in the range $[0,1]$ like $E_{0x}(\phi_a,\phi_b)$, because of the discussed above polarization sensitive efficiency of the grating. In consequence, Equations 2.15 from Section 2.2 cannot be applied, since for some set of parameters (I,r,γ) they return $E_{0y}(I,r,\gamma)=1$, which cannot be reached in case of $E_{0y}(\phi_a,\phi_b)$. However, this problem can be circumvented by comparing not the amplitudes but their ratio

$$\frac{E_{0y}(\phi_a,\phi_b)}{E_{0x}(\phi_a,\phi_b)}=\frac{E_{0y}(I,r,\gamma)}{E_{0x}(I,r,\gamma)}$$

which yields

$$\phi_b = \arctan \sqrt{\frac{(1 + r^2 - \cos(2\gamma) + r^2 \cos(2\gamma))}{((1 + r^2 + \cos(2\gamma) - r^2 \cos(2\gamma))g^2)}} \,. \tag{5.12}$$

Since the gratings have influenced the intensity as well, it has to be taken into account when calculating the overall transmission. Fortunately, this problem is identical as for the case of the serial shaper.

$$\phi_a = \arccos \sqrt{\frac{T\,g}{\cos^2(\frac{\phi_b}{2}) + g \sin^2(\frac{\phi_b}{2})}} \tag{5.13}$$

The phase and relative phase shift between the polarization component remains unaffected by the grating.

$$\varphi = \frac{1}{2}(\phi_a + \phi_b + \phi_c + \phi_d) \tag{5.14}$$

$$\phi_c - \phi_d = \epsilon - \frac{\pi}{2} =$$

$$= \pm \frac{\sin(\gamma)}{|\sin(\gamma|} \arccos \sqrt{\frac{r^2 - 1}{1 + r^4 + r^2(\cot^2(\gamma) + \tan^2(\gamma))}} - \frac{\pi}{2} \tag{5.15}$$

The presented Equations 5.12, 5.13, 5.14 and 5.15 determine the retardances for the desired phase, amplitude, and polarization states of the electromagnetical wave. An analogical equation can be found for the three pass setup.

5.4 Summary

Chapter 5 is a theoretical addition to Chapter 4 and it discusses the possibility of combining liquid crystal arrays with $\pm 45°$, $0°$ and $90°$ orientated optical axes in order to circumvent restrictions in polarization shaping. Then practical solutions are proposed by designing new crystals sandwiches by utilizing commercially accessible modulators.

First, the interaction of light with arbitrary orientation is studied. The conclusion is drawn, that in order to be able to change the amplitudes of orthogonal polarization components in full range, the optimal orientation is

$\pm 45°$. In order to achieve this together with phase control for both polarization components independently, additional $0°$ and $90°$ orientated arrays are needed. Then, the full phase and polarization control can be achieved with $\pm 45°$, $0°$ and $90°$. The missing amplitude control is attained by adding $\pm 45°$ arrays and a $0°$ orientated polarizer. This way a modulator that is capable of full control over the phase, amplitude, and polarization is designed. Next, accomplishing the same effect with the use of a three pass shaper with properly aligned waveplates is discussed. At the end, the retardances of the four array modulator are calculated as a function of the polarization ellipse and absolute phase including the grating polarization sensitive efficiency.

The presented four layer modulator is technologically not much more advanced than commercially available modulators and can be a simple tool to achieve full control over the femtosecond pulse structure.